Two-photon emission in coupled biexciton quantum dot–cavity system: Phonon-assisted model*

Peng Yi-Wei(彭益炜), Yu Zhong-Yuan(俞重远)†, Liu Yu-Min(刘玉敏), Wu Tie-Sheng(伍铁生), and Zhang Wen(张 文)

State Key Laboratory of Information Photonics and Optical Communications (Beijing University of Posts and Telecommunications), Beijing 100876, *China*

(Received 23 May 2014; revised manuscript received 30 June 2014; published online 10 October 2014)

We theoretically analyze the steady state emission spectrum and transient temporal dynamics in a coupled biexciton quantum dot (QD)–cavity system. For steady state, a phonon-assisted biexciton–exciton cascade model under continuous wave (CW) excitation is presented to explain the asymmetric QD–cavity emission spectrum intensities (intensities of cavity, exciton, and biexciton emission peak) in off-resonance condition. Results demonstrate that the electron–phonon process is crucial to the asymmetry of emission spectrum intensity. Moreover the transient characteristics of the biexciton–exciton cascade system under pulse excitation show abundant nonlinear temporal dynamic behaviors, including complicated oscillations which are caused by the four-level structure of QD model. We also reveal that under off-resonance condition the cavity outputs are slightly reduced due to the electron–phonon interaction.

Keywords: biexciton–exciton cascade, phonon, emission spectrum, temporal dynamic

PACS: 42.50.Pq, 78.67.Hc, 42.50.Ct **DOI:** 10.1088/1674-1056/23/12/124204

1. Introduction

Semiconductor quantum dots coupled to microcavities, derived from cavity quantum electrodynamics (CQED), are usually used for investigating the interaction between light and matter.[1,2] Mollow triplet, entangled photons, and other phenomena in solid state systems have widely been studied in recent years both theoretically and experimentally, showing that the electron–phonon process plays an important role.[3–6]

A pair of photons emitted simultaneously, referred to as two-photon emission, has a variety of applications in two-photon lasing,[7] photon source,[8] and spin initialization.[9] Elena *et al*. theoretically investigated the creation conditions of two-photon lasing.[7] Lin *et al*. used two-photon emission to generate single photon and entangled photon pairs.[8] Arka *et al*. adopted the two-photon process to obtain trion state and realized spin initialization under the condition of no strong magnetic field.[9] Alex *et al*. introduced the novel applications of the two-photon process in semiconductors.[10] In the recent experiments the two-photon spontaneous emission has proved to exist in a system where a QD is embedded in a microcavity.[11] However, when the simulation results are compared with the experimental results, the distinctions in the symmetric emission spectrum show that some physical processes are missing in the theory model. Therefore electron–phonon interaction is considered in this work to explain the distinctions.

Arka *et al*. theoretically and experimentally analyzed the temporal dynamics of QD–cavity system under pulse excitation.[12] After the pulse excitation of the system, an oscillation in the cavity output, which is due to the interaction between QD and cavity, is observed. This oscillation would vanish as the coupling between QD and cavity decreases. For a biexciton–exciton cascade system, relevant work on the temporal dynamics is lacking. Besides, the influence of phonons which might affect the results is ignored in the proposed model.

In this work we take electron–phonon into consideration to study the biexciton–exciton cascade system, proving that phonons break the symmetric structures of cavity, exciton, and biexciton emission peak intensities. The temporal dynamic behaviors of the coupled system under optical pulse excitation are analyzed, and effects of pulse width and electron–phonon interaction are also investigated. The rest of this paper is organized as follows. In Section 2 the basic model and simulation method of the coupled QD–cavity system are introduced. In Section 3 the steady state emission spectrum of phonon-assisted system and temporal dynamics under pulse excitation are demonstrated. Finally some conclusions are drawn from the present studies in Section 4.

2. Basic model and method

The system to be considered here is composed of a QD embedded in a single mode photonic-crystal cavity.[11] Figures 1(a) and 1(b) show the energy-level diagrams for the no-phonon-assisted and phonon-assisted biexciton–exciton cas-

*Project supported by the National Natural Science Foundation of China (Grant Nos. 61275201 and 61372037), the Beijing Municipal Excellent Ph. D. Thesis Guidance Foundation (Grant No. 20131001301), and the Fund of State Key Laboratory of Information Photonics and Optical Communications (Beijing University of Posts and Telecommunications), China.

†Corresponding author. E-mail: yuzhongyuan30@gmail.com

© 2014 Chinese Physical Society and IOP Publishing Ltd

cades respectively. The biexciton state $|B\rangle$ has two kinds of decay routes: (i) one is that the state first decays to two orthogonal polarization exciton states $|X\rangle$, $|Y\rangle$ with a fine structure splitting δ existing between them, then decays to the ground state $|G\rangle$, emitting one photon in each transition; (ii) biexciton state $|B\rangle$ decays directly to ground state $|G\rangle$, emitting two photons. Frequencies of these four states and cavity are $2\omega_X - \chi$, ω_X, ω_Y, 0, and ω_C respectively, with χ being the binding energy. As explained in the experiment,[11] we assume that the cavity mode only couples with transitions via $|X\rangle$.

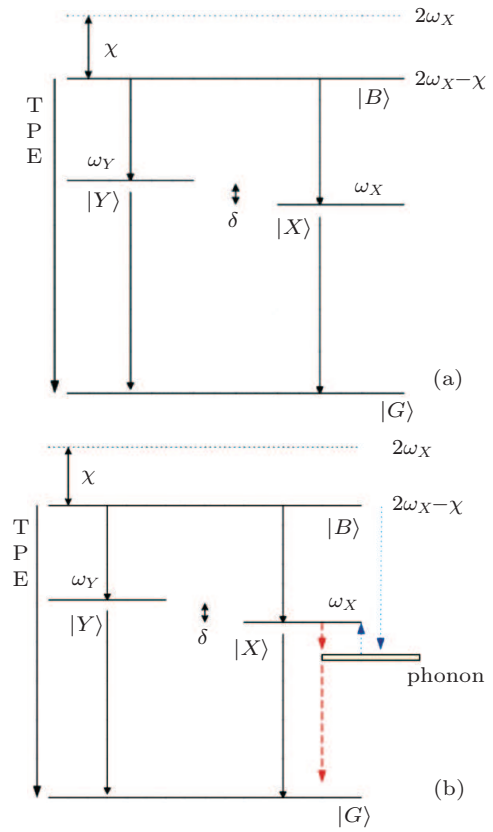


Fig. 1. (color online) Four-level diagrams for (a) no-phonon-assisted and (b) phonon-assisted biexciton–exciton cascades. For our new model two transitions are marked by dashed and dotted arrows, and the roles of phonon in the coupled system are indicated.

We note that several methods have been proposed to study the influence of phonon interaction,[13–17] and in this work we adopt the phonon-assisted model[18] to analyze the role of the phonon. The effects of the phonon can be modeled by adding a virtual state into the coupled QD–cavity system, which means adding several additional incoherent decay terms into the master equation. The added transitions via the new virtual state are marked by dashed and dotted arrows in Fig. 1(b). Now the phonon-assisted transitions emit or absorb photons by emitting or absorbing phonons. Taking transition $|X\rangle \to |G\rangle$ for example, the exciton state first decays to the virtual state through creating phonons, then decays to a ground state through creating a photon. For the photon annihilation process, it is a contrary process. Similar processes occur in a cavity-assisted atomic decay system.[19] We also notice that several groups have proposed phonon-assisted models under QD–cavity off-resonance condition.[20–25] In their work alternative effective master equations with phonon-modified scattering rate are proposed, introducing extra exciton–cavity terms, which are consistent with our model in form. As only transitions via $|X\rangle$ couple with cavity, the phonon-mediated couplings via $|X\rangle$ are much stronger than those via $|Y\rangle$, which means that the phonon-assisted transitions via $|Y\rangle$ are ignored.

We use the master equation method to numerically calculate the coupled system. Using the rotating-wave approximation and taking rotating frame at the $|X\rangle \to |G\rangle$ transition frequency ω_X, the master equation is[1,11,18]

$$\dot{\rho} = -\mathrm{i}\,[H,\rho] + L\rho + L_{\text{phonon}}\rho. \tag{1}$$

The Hamiltonian of the system is given as

$$\begin{aligned} H \;=\; & -\chi\sigma_{BB} + \delta\sigma_{YY} + \delta_C a^\dagger a + g_X(\sigma_{GX}a^\dagger + \text{H.C.}) \\ & + g_B(\sigma_{XB}a^\dagger + \text{H.C.}), \end{aligned} \tag{2}$$

where σ_{ij} is the transition operator representing $|i\rangle\langle j|$, $\delta_C = \omega_C - \omega_X$ is the detuning between cavity frequency and exciton frequency, a and $a^\dagger$ are the annihilation and creation operators of the cavity mode, and g_X and g_B are the coupling strengths between cavity and QD. Including cavity loss rate κ, QD spontaneous emission rate γ, incoherent pumping rate P and pure dephasing rate γ_{phase}, we obtain the expression of incoherent process $L\rho$:

$$\begin{aligned} L\rho \;=\; & \kappa\mathcal{L}(a)\rho + \gamma[\mathcal{L}(\sigma_{XB})\rho + \mathcal{L}(\sigma_{YB})\rho + \mathcal{L}(\sigma_{GX})\rho \\ & + \mathcal{L}(\sigma_{GY})\rho] + P[\mathcal{L}(\sigma_{BX})\rho + \mathcal{L}(\sigma_{BY})\rho + \mathcal{L}(\sigma_{XG})\rho \\ & + \mathcal{L}(\sigma_{YG})\rho] + \gamma_{\text{phase}}[2\mathcal{L}(\sigma_{BB})\rho \\ & + \mathcal{L}(\sigma_{XX})\rho + \mathcal{L}(\sigma_{YY})\rho], \end{aligned} \tag{3}$$

where $\mathcal{L}(x)$ is the Lindblad operator defined as[17]

$$\mathcal{L}(x)\rho = x\rho x^\dagger - \frac{1}{2}x^\dagger x\rho - \frac{1}{2}\rho x^\dagger x.$$

For the phonon-induced term, we define it as follows (see also Ref. [18]):

$$L_{\text{phonon}}\rho \;=\; \begin{cases} \gamma_{\text{ph}}(n+1)\mathcal{L}(\sigma_{XB}a^\dagger)\rho + \gamma_{\text{ph}}n\mathcal{L}(\sigma_{BX}a)\rho + \gamma_{\text{ph}}n\mathcal{L}(\sigma_{GX}a^\dagger)\rho + \gamma_{\text{ph}}(n+1)\mathcal{L}(\sigma_{XG}a)\rho, & \delta_C > 0, \\ \gamma_{\text{ph}}(n+1)\mathcal{L}(\sigma_{BX}a)\rho + \gamma_{\text{ph}}n\mathcal{L}(\sigma_{XB}a^\dagger)\rho + \gamma_{\text{ph}}n\mathcal{L}(\sigma_{XG}a)\rho + \gamma_{\text{ph}}(n+1)\mathcal{L}(\sigma_{GX}a^\dagger)\rho, & \delta_C < 0, \end{cases} \tag{4}$$

where $\gamma_{\rm ph}$ is the introduced effective decay rate, and $n = (e^{\hbar|\delta_C|/k_B T} - 1)^{-1}$ is the average number of phonons under cavity–QD detuning and temperature.

We simulate the QD–cavity system with the experimental parameters cited from Ref. [11], which are coupling strengths $g_X = 51$ μeV and $g_B = 43$ μeV, cavity loss rate $\kappa = 24$ μeV, binding energy $\chi = 400$ μeV, QD decay rate $\gamma = 0.13$ μeV, incoherent pumping rate $P = 0.05$ μeV, pure dephasing rate $\gamma_{\rm phase} = 30$ μeV, and temperature $T = 4$ K, and we introduce the additional decay rate $\gamma_{\rm ph} = 0.22$ μeV. This phonon-related value $\gamma_{\rm ph}$ represents the electron–phonon interaction and normally has the same magnitude as the pure dephasing rate if $\gamma_{\rm phase}$ is ignored.[18] Therefore in order to obtain $\gamma_{\rm ph}$ in this paper, we use different values from 0 to pure dephasing rate to calculate the emission spectra, by choosing the values that match the experimental data best. Some functions in quantum optics toolbox[26] are cited in the present study.

3. Results and discussion

3.1. Steady state spectrum

Under incoherent pumping, the emission spectrum $S(\omega)$ of the QD–cavity coupling system in a steady state is composed of two parts: one is about the photon emission via the radiation of the microcavity $S_C(\omega)$, and the other part is about the photon emission via the radiation of QD $S_X(\omega)$. Using quantum regression theorem, the emission spectrum is evaluated from the formula[27–30]

$$\begin{aligned} S(\omega) &= S_C(\omega) + S_X(\omega) \\ &\propto \lim_{t\to\infty} \mathrm{Re}\left\{ \kappa \int_0^\infty \langle a^\dagger(t) a(t+\tau)\rangle \, e^{i\omega\tau} d\tau \right. \\ &\quad + \gamma \int_0^\infty [\langle \sigma_{XB}^\dagger(t)\sigma_{XB}(t+\tau)\rangle \\ &\quad \left. + \langle \sigma_{GX}^\dagger(t)\sigma_{GX}(t+\tau)\rangle] e^{i\omega\tau} d\tau \right\}. \end{aligned} \tag{5}$$

It should be noted that the difference in detection efficiency between the cavity and QD emission channel are ignored in the spectrum calculation.

Figure 2(a) shows the emission spectra of the system in two-photon resonance $\omega_C - \omega_X = -\chi/2 = -200$ μeV with and without phonon interaction. In this subsection exciton frequency is fixed while the cavity resonant frequency is varying. The three peaks around −400 μeV, −200 μeV, and 0 μeV represent the emissions of biexciton (biexciton-to-exciton transition), cavity, and exciton (exciton-to-ground state transition) respectively. In the two-photon resonance, the biexciton emissions are suppressed and two-photon emission process reaches a maximum. It can be observed that the biexciton emission line around −400 μeV is nearly zero and the amplitudes of cavity emission and exciton emission are influenced by the phonon evidently. Owing to incoherent dot pumping, the processes, which create a cavity photon and collapse QD to a lower state, are represented by the decay term $\sigma_{ij}a^\dagger$ in the phonon-induced Lindblad operator $L_{\rm phonon}\rho$ and play an important role in cavity emission.[17] Thus it is observed in Fig. 2(a) that the cavity emission is enhanced while exciton emission is reduced.

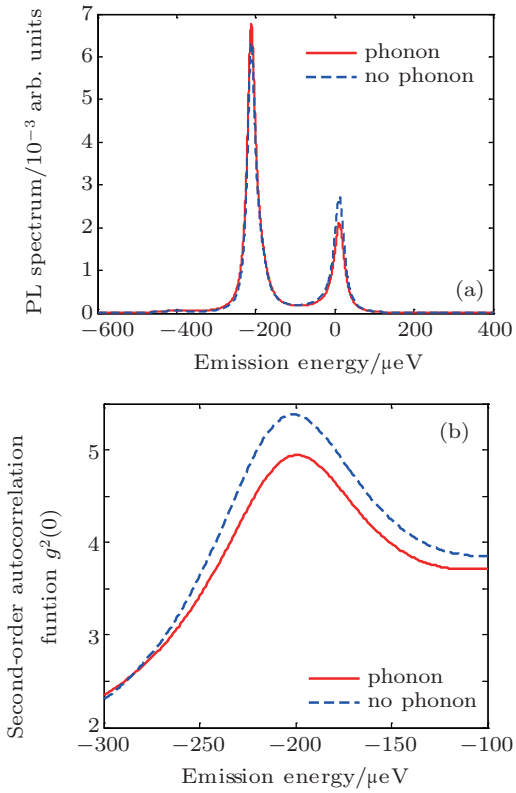


Fig. 2. (color online) (a) Emission spectra under two-photon resonance $\omega_C - \omega_X = -\chi/2 = -200$ μeV, with (solid curve) and without (dashed curve) photon interaction. In this condition biexciton–exciton transition is suppressed most. (b) Second-order autocorrelation function $g^2(0)$ under different values of cavity detuning $\omega_C - \omega_X$ (-300 μeV ~ -100 μeV) and pump rate $P = 1$ μeV, with (solid curve) and without (dashed curve) photon interaction.

Figure 2(b) shows the calculated values of second-order autocorrelation function $g^2(0)$ under different values of cavity detuning $\omega_C - \omega_X$. The photon number space is truncated at $N = 4$ under low excitation $P = 1$ μeV. We observed bunching phenomena ($g^2(0) > 1$) which indicate a two-photon emission process, and the largest probability appears around cavity detuning -200 μeV ($g^2(0) \approx 4.8$), which is the two-photon resonance condition. In the phonon-assisted situation the second-order function is similar to that in the case of no photon interaction, with the magnitude declining. These results would be a supplement in relevant work like the GaN QD case.[31]

Next, the emission spectra of a phonon-assisted model under several cavity–exciton detunings are calculated and shown in Fig. 3, and the intensities of cavity, exciton, and biexciton emissions are extracted and plotted in Figs. 4(a) and 4(b) respectively. We observe that biexciton emissions are much smaller than cavity and exciton emissions that are plotted in an independent figure. Compared with the experimental

data[11] and numerical calculations, our phonon-assisted results agree with the experimental results well. For the case without phonon interaction, the cavity and exciton emission intensities are symmetric for the two-photon resonance frequency −200 μeV, which is also claimed in Ref. [11]. After considering phonon-assisted transitions, this situation is changed. The cavity emission intensities are enhanced due to the cavity-feeding effects induced by the phonon under cavity–exciton detuning; however under different detunings the average numbers of phonons n are different. Therefore an asymmetric structure of cavity emission intensity is formed with considering the influence of phonon. For the exciton intensity, it is a contrary process.

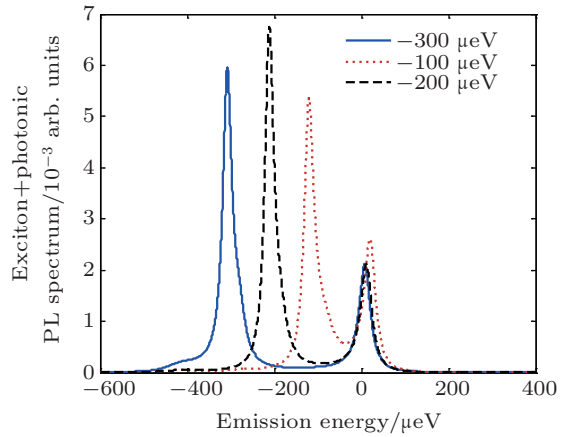


Fig. 3. (color online) Emission spectra under different exciton–cavity detunings. We choose three different values of critical detuning $\omega_C - \omega_X = -100$ μeV (dotted curve), $\omega_C - \omega_X = -200$ μeV (dashed curve), and $\omega_C - \omega_X = -300$ μeV (solid curve) to cover a large detuning range and have a general knowledge of the changing trend of emission spectrum.

The shortcoming of our result is that the phonon method we have used is suited only for QD–cavity off-resonance condition. When QD and cavity are in resonance or in small detuning our theory is inapplicable, which can be seen if we compare our numerical results with experimental data[11] under the condition of QD–cavity detuning −100 μeV. In the experiment the cavity and exciton intensities are nearly equal while in our case large difference exists between them. The reason is that the phonon-assisted method we used is in a Markovian way, and electron–phonon interactions are only included to first-order.[25] In the large QD–cavity detuning, higher-order phonon effects can be ignored, however in the small detuning a non-Markovian method is needed to obtain accurate higher-order electron–phonon interactions.[15,23] But this process could be complex and tedious, therefore in this work we treat the electron–phonon interaction by a simplified method,[18] which is consistent with the results obtained in the large off-resonance condition. This method can explain the interaction in some aspects and the calculation processes are much reduced. To obtain a full knowledge of the phonon role in the two-photon process, a non-Markovian description should be considered in the future work.

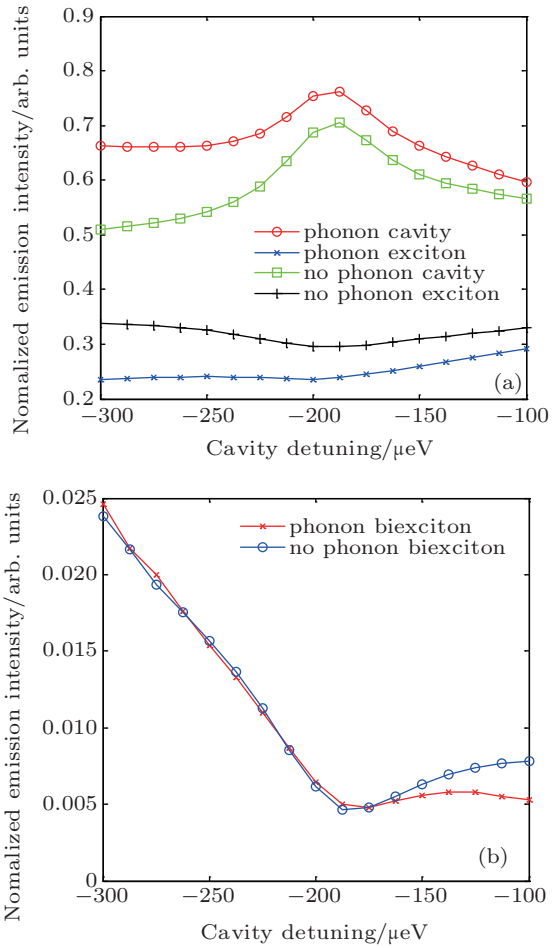


Fig. 4. (color online) Effects of phonons on the intensities of emission lines: (a) exciton and cavity emission; (b) biexciton emission under detunings varying from −100 μeV to −300 μeV. Biexciton emissions are too small compared with other emission lines, thus they are shown in an independent figure.

3.2. Temporal dynamics

We use the master equation and Monte Carlo wavefunction method (MCWFM)[32] to calculate the transient results of the QD–cavity coupling system, thus coherent cavity pumping instead of incoherent pumping is taken into account. First we consider a simple case where pure dephasing and phonon interaction are ignored, which means that the master equation reduces to the following form:

$$\begin{aligned}\dot{\rho} &= -\mathrm{i}[H^{\mathrm{T}},\rho] + \kappa\mathcal{L}(a)\rho + \gamma[\mathcal{L}(\sigma_{XB})\rho \\ &\quad + \mathcal{L}(\sigma_{YB})\rho + \mathcal{L}(\sigma_{GX})\rho + \mathcal{L}(\sigma_{GY})\rho], \qquad (6)\\ H^{\mathrm{T}} &= -\chi\sigma_{BB} + \delta\sigma_{YY} + \delta_C a^\dagger a + g_X(\sigma_{GX}a^\dagger + \mathrm{H.C.}) \\ &\quad + g_B(\sigma_{XB}a^\dagger + \mathrm{H.C.}) + \Omega(t)(a + a^\dagger), \qquad (7)\end{aligned}$$

where $\Omega(t) = \Omega_0 \exp[-(2\sqrt{\ln 2})^2(t-\tau_0)^2/\tau_{\mathrm{fwhm}}^2]$ is the excitation Gaussian pulse envelope, Ω_0 is the pulse amplitude, τ_0 is the center of the pulse, and τ_{fwhm} is the full width at half maximum (FWHM).

The cavity outputs $(\kappa a^{\dagger}a)$ in arbitrary units under pulse excitation are shown in Fig. 5(a). The pulse-related parameters are $\Omega_0 = 1$ μeV, $\tau_{\rm fwhm} = 5$ ps, which ensure that the system is in the low excitation limit, and other parameters are the same as those in Fig. 2. Figure 5(b) shows the case of smaller coupling strengths, namely $g_X = 51/2$ μeV and $g_B = 43/2$ μeV. We reveal two main results: i) a strong oscillation in the cavity output exists due to the Rabi oscillation of photons between QD and cavity; ii) the oscillation fades as coupling constants g_X and g_B decrease.[12] The first peak in cavity output is expanded by nearly twice the excitation pulse while in a two-level QD model case it remains the same. We attribute the expanding peak to being due to the four-level structure of QD enlarging the energy exchanging time.

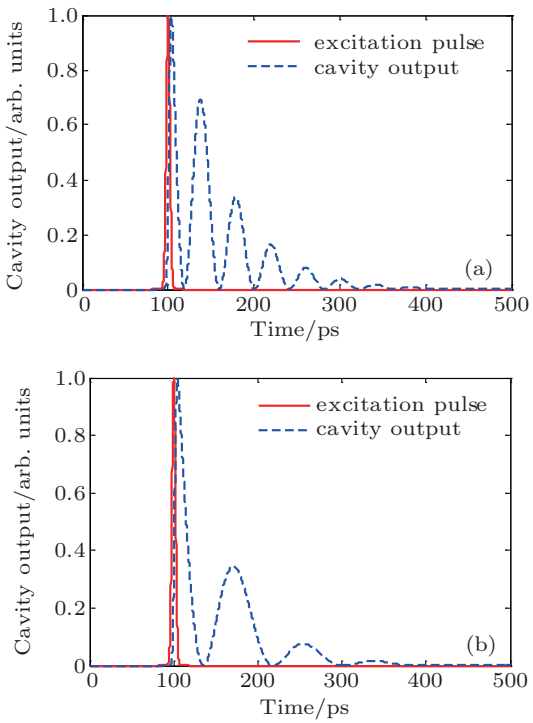


Fig. 5. (color online) (a) Cavity outputs in arbitrary units under cavity–exciton resonance condition ($\omega_C - \omega_X = 0$), with excitation pulse denoted by solid line, and normalized cavity output by dashed line. ($g_X = 51$ μeV, $g_B = 43$ μeV). (b) Cavity outputs with different coupling strengths ($g_X = 51/2$ μeV, $g_B = 43/2$ μeV), with excitation pulse denoted by solid line and normalized cavity output by dashed line. In both cases phonon and pure dephasing are ignored, and other parameters are the same as those in Fig. 2.

The effects of pulse width on the cavity output are shown in Fig. 6, where the temporal dynamic properties under various FWHMs are calculated. When the FWHM differs from 5 ps to 50 ps, oscillation frequency decreases, which is like the QD–cavity system where QD is regarded as a two-level system. However the oscillation amplitudes increase and then decrease with the increase of pulse width. To explain this, we calculate the steady state spectrum of this biexciton–exciton cascade system in exciton–cavity resonance (Fig. 7). There are four eigenvalues of the coupled system, where X_1 and X_2 are located around biexciton energy, and X_3 and X_4 are located around excition energy. For 5-ps pulse, its bandwidth is large enough to modulate all these four eigenvalues, however X_1 and X_2 are much smaller than X_3 and X_4 which reduce amplitudes; for 30-ps pulse, its bandwidth is only large enough to modulate with X_3, X_4; for 50-ps pulse, its bandwidth is too narrow to modulate with either of these four eigenvalues, which leads to the decreasing of oscillation amplitude.

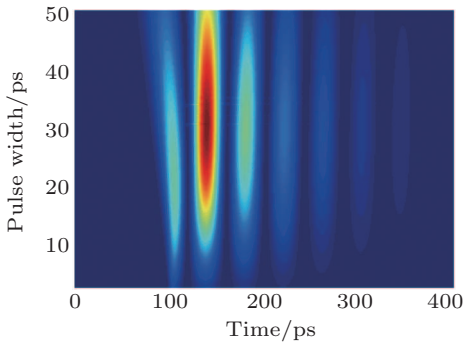


Fig. 6. (color online) Relationships between cavity output and pulse FWHM, where the FWHM of pulse changes from 5 ps∼ 50 ps and other parameters are the same as those in Fig. 5.

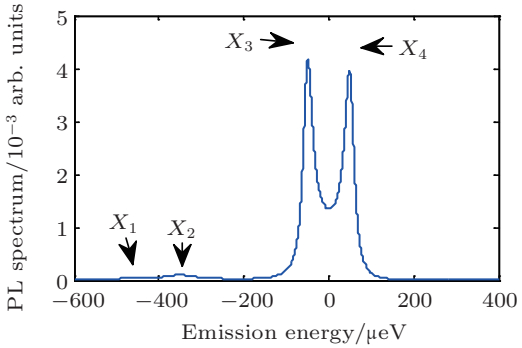


Fig. 7. (color online) Steady state photon-luminescence (PL) spectrum in exciton–cavity resonance under CW excitation. Four eigenvalues are denoted as X_1, X_2, X_3, and X_4 in the plot.

In the above calculations temporal dynamic properties without phonon interaction are shown, and the phonon interaction is considered in the two-photon resonance. Therefore the pure dephasing term and phonon-induced term mentioned in the former spectrum case are added. The cavity outputs with and without phonon interaction are compared in Fig. 8, where phonon-related parameters are $\gamma_{\rm phase} = 30$ μeV and $\gamma_{\rm ph} = 0.22$ μeV, and other system parameters are the same as those in Fig. 5. In the phonon-assisted case smaller amplitudes of cavity output than in the no-phonon-assisted case are observed. We explain the reduced cavity output as phonons enhancing the cavity emission, thereby lowering the cavity photons; therefore the cavity output which is proportional to $(\kappa a^{\dagger}a)$ decreases in the phonon-assisted case. However the effects of phonon on temporal dynamics are extremely weak. One reason may be that the interaction between QD and cav-

ity decreases with the increase of the detuning between exciton and cavity, which leads to the reduction of oscillation frequency and amplitude. Since the total change is small, positive phonon influence becomes slighter.

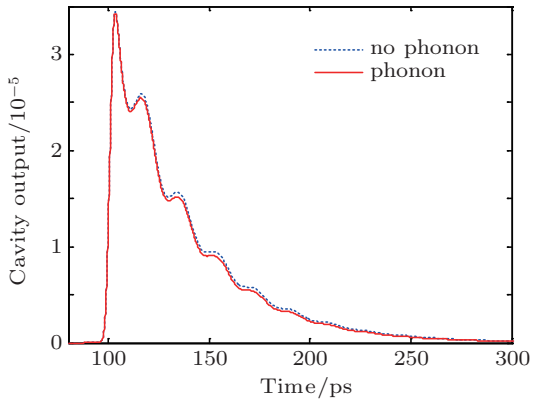


Fig. 8. (color online) Influences of phonon on cavity output in the time domain under two-photon resonance; phonon-assisted model (solid line) and model without phonon (dashed line). Phonon-related parameter is $\gamma_{ph} = 0.22$ μeV, and others parameters are the same as those in Fig. 5.

4. Conclusions

In this paper, the emission spectra of phonon-assisted two-photon emission are numerically calculated and compared with experimental results. It is demonstrated that the electron–phonon process plays an important role in the two-photon emission process by breaking the symmetric structures of emission intensities and changing the amplitudes of luminescence spectra. The temporal dynamics of biexciton–exciton cascade system under Gaussian pulse excitation is analyzed and a complex oscillation is revealed. The quenching time of this oscillation is one order of magnitude longer than the calculation from the two-level QD model.[12] After pulses with different FWHM values exciting the system, the variations of cavity outputs are non-monotonic. We also prove that the time-domain phonon-assisted cavity outputs are reduced compared with no-phonon-assisted cavity outputs under off-resonant condition.

References

[1] Marlan O S and Muhammad S Z 1997 *Quantum Optics* (Cambridge: Cambridge University Press)
[2] Hennessy K, Badolato A, Winger M, Gerace D, Atature M, Gilde S, Falt S, Hu E L and Lmamoglu A 2007 *Nature* **445** 896
[3] Luo Z H 2013 *Acta Phys. Sin.* **62** 207201 (in Chinese)
[4] Hai L, Tan L, Feng J S, Xu W B and Wang B 2014 *Chin. Phys. B* **23** 024202
[5] Zhang Y Y, Chen Q H and Zhu S Y 2013 *Chin. Phys. Lett.* **30** 114203
[6] Shu C G, Xin X, Liu Y M, Yu Z Y, Yao W J, Wang D L and Cao G 2012 *Chin. Phys. B* **21** 044208
[7] Elena D V, Stefano Z, Fabrice P L, Alejandro G T, Giovanna M and Carlos T 2010 *Phys. Rev. B* **81** 035302
[8] Lin Z L and Jelena V 2010 *Phys. Rev. B* **81** 035301
[9] Arka M, Lin Z L, Andrei F and Jelena V 2010 *Phys. Rev. A* **82** 022301
[10] Alex H, Amir N, Pavel G and Meir O 2011 *Semicond. Sci. Technol.* **26** 083001
[11] Yasutomo O, Satoshi I, Naoto K and Yasuhiko A 2011 *Phys. Rev. Lett.* **107** 233602
[12] Arka M, Dirk E, Michal B and Jelena V 2012 *Phys. Rev. A* **85** 033802
[13] Roy C and Hughes S 2011 *Phys. Rev. Lett.* **106** 247403
[14] Luker S, Gawarecki K, Reiter D E, Grodecka G A, Axt V M, Machnikowski P and Kuhn T 2012 *Phys. Rev. B* **85** 121302
[15] Kaer P, Nielsen T R, Lodahl P, Jauho A P and Mørk J 2010 *Phys. Rev. Lett.* **104** 157401
[16] Wilson-Rae I and Imamoğlu A 2002 *Phys. Rev. B* **65** 235311
[17] Chen Q, Wang H L, Wang H, Gong Q and Song Z T 2013 *Acta Phys. Sin.* **62** 226301 (in Chinese)
[18] Arka M, Erik D K, Gong Y Y, Michal B and Jelena V 2011 *Phys. Rev. B* **84** 085309
[19] Ulrich H, Arne L, Michael K, Norman H, Andre N, Abbas M, Marek S, Max B and Jonathan J F 2009 *Phys. Rev. B* **80** 201311
[20] Gangopadhyay G, Basu S and Ray D S 1993 *Phys. Rev. A* **47** 1314
[21] Xue J, Zhu K D and Zheng H 2008 *J. Phys.: Condens. Matter* **20** 325209
[22] Ulrich H 2010 *Phys. Rev. B* **81** 155303
[23] Roy C and Hughes S 2012 *Phys. Rev. B* **85** 115309.
[24] Dara P S M, Nikesh S D, Erik M G, Brendon W L and Ahsan N 2011 *Phys. Rev. B* **84** 081305
[25] Roy C and Hughes S 2011 *Phys. Rev. X* **1** 021009
[26] Lindblad G 1976 *Commun. Math. Phys.* **48** 119.
[27] Sze M T 1999 *J. Opt. B: Quantum Semiclass. Opt.* **1** 424
[28] Fabrice P L, Laucht A, Elena d V, Finley J J and Villas-Bôas J M 2011 *Phys. Rev. B* **84** 195313
[29] Yasutomo O, Satoshi I, Naoto K and Yasuhiko A 1999 arXiv: 0908.0788
[30] Natsuko I, Tim B, Franco N and Yoshihisa Y 2013 *Sci. Rep.* **3** 1180
[31] Callsen G, Carmele A, Honig G, Kindel C, Brunnmeier J, Wagner M R, Stock E, Reparaz J S, Schliwa A, Reitzenstein S, Knorr A and Hoffmann A 2013 *Phys. Rev. B* **87** 245314
[32] Klaus M, Yvan C and Jean D 1993 *J. Opt. Soc. Am. B* **10** 524